Interaction of a high-intensity relativistic electron beam with plasma in a magnetic field

Yu. I. Abrashitov, V. S. Koĭdan, V. V. Konyukhov, V. M. Lagunov, V. N. Luk'yanov, K. I. Mekler, and D. D. Ryutov

Institute of Nuclear Physics, Siberian Branch, USSR Academy of Sciences
(Submitted October 10, 1973)
Zh. Eksp. Teor. Fiz. **66**, 1324–1337 (April 1974)

Results are reported of experiments on the interaction between a high-intensity relativistic electron beam (electron energy 1 MeV, current 5 kA, pulse length 70 nsec) with plasma (density 3×10^{14} cm^{-3}) in a magnetic field of up to 15 kOe. The behavior of the beam both in vacuum and in plasma was investigated. It was found that when the beam passed through plasma with density $n < 10^{13}$ cm^{-3} there was a substantial axially nonsymmetric spreading of the beam. Possible reasons for this phenomenon are discussed. It was established that up to densities $n \sim 2 \times 10^{14}$ cm^{-3} there was no observable collisionless heating of the plasma by the electron beam with an efficiency of 10–15%. It is shown that at least for densities $n \gtrsim 5 \times 10^{13}$ cm^{-3} the heating of the plasma may be connected with the development of two-stream instability on Langmuir oscillations. The compensation of the beam current by the reverse plasma current is also investigated for different plasma densities.

1. INTRODUCTION

The experiments described in[1] were the first to demonstrate the presence of an appreciable collective interaction between a high-current relativistic electron beam and plasma. In these experiments, the beam density was $n_b \approx 5 \times 10^{10}$ cm^{-3} and the electron energy was $E_b = 2-3$ MeV. The beam was injected into plasma of density $n = 10^{11}-10^{14}$ cm^{-3} in a longitudinal magnetic field $H = 1-2$ kOe. It was found that, under certain definite conditions, an appreciable fraction ($\sim 10\%$) of the initial beam energy was transferred to the plasma.[1] This can only be explained by collective effects because, under the conditions of the experiment described in[1], the Coulomb mean free paths of both the beam and plasma electrons were much greater than the length of the installation.

The energy transferred to the plasma was very dependent on the plasma density: it was a maximum for $n \sim 10^{12}$ cm^{-3} and fell rapidly both when the plasma density was reduced and increased (the latter is the more important). Theory[1,2] shows that the plasma heating efficiency can be increased for large n by increasing the particle density n_b in the beam, by reducing the particle energy E_b (down to $E_b \sim mc^2$), and by increasing the longitudinal magnetic field H. The INAR installation was constructed on the basis of these ideas.[3] It has the following parameters: the particle density in the beam has been increased up to $\sim 5 \times 10^{11}$ cm^{-3} at beam energies of the order of 1 MeV and the longitudinal magnetic field has been increased up to 15 kOe.

Physical data obtained with the INAR installation are reported below.

2. APPARATUS AND METHODS OF MEASUREMENT

The apparatus is shown schematically in Fig. 1. The electron beam with initial energy of ~ 1 MeV, beam current 5 kA, and pulse length 50–70 nsec was generated by a pulsed electron accelerator. The energy bank 1 (cylindrical capacitor of ~ 500 pF) was charged to ~ 1.5 MV by a pulse transformer. When the voltage across the bank reached its maximum value, the discharge gap 2 broke down, and the voltage was applied across the vacuum diode 4. The field-emission cathode was a stainless steel, thin-walled, hollow cylinder with a flat end and a diameter of 2 cm.
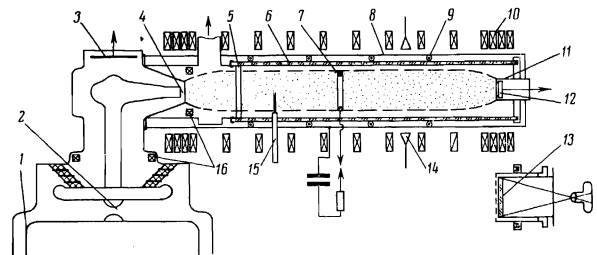

FIG. 1. The experimental installation: 1—energy bank, 2—discharge gap, 3—capacitative divider, 4—vacuum diode, 5—quartz diaphragm, 6—discharge chamber, 7—Penning anode, 8—reverse current leads, 9—diamagnetic probes, 10—magnetic field coils, 11—exit electrode, 12—calorimeter and shunt, 13—plasmoscope, 14—microwave horns, 15—double probes, 16—Rogowski belts.

The main part of the vacuum chamber 6 was in the form of a glass tube with an internal diameter of 11 cm and length 220 cm. It was joined to the end of the accelerator by a stainless steel union (wall thickness ~ 1 mm). Titanium foils, 50 μ thick, were mounted at both ends of the vacuum chamber, and one of them was used as the accelerator anode. The beam passing through the vacuum chamber was received by the exit electrode 1 which was connected to the accelerator by four current return leads 8 located on the outer surface of the glass tube.

The quasistationary magnetic field had a mirror geometry (mirror ratio 1.7) and was produced by the solenoid 10 with an internal diameter of 20 cm. The distance between the mirrors was 230 cm. The maximum magnetic field at the center of the installation was 15 kOe and was uniform to better than 1%.

The preliminary hydrogen plasma was generated by a pulsed Penning discharge. The entrance and exit foils, 6 cm in diameter, located in the magnetic mirrors, served as the discharge cathodes. The anode was the ring 7 with a diameter of 8 cm, placed at the center of the vacuum chamber. A positive voltage of ~ 20 keV supplied by the capacitor bank was applied to the discharge anode. The 5–10 kA discharge current with a pulse length of 10–15 μsec produced a plasma column 8–9 cm in diameter with plasma density up to $3 \times 10^{14}-4 \times 10^{14}$ cm^{-3} and degree of ionization of about 50%. The electron temperature in the preliminary plasma, measured with the electric double probe 15, was 2–3 eV.

By varying the time of injection of the beam relative to the preliminary discharge, it was possible to select the necessary plasma density. To eliminate the effect of the current in the Penning discharge on the beam dynamics, the beam was injected into the plasma at least 10 to 20 μsec after the end of the discharge current.

The voltage on the field emission cathode in the accelerator was measured with the capacitive divider 3. The current in the cathode circuit and the total current in the plasma was measured by the Rogowski belts 16. The beam current at exit from the plasma, and the total energy transported by the beam per pulse, were measured with a shunt and a graphite calorimeter,[2] respectively, which were combined in the single unit 12. In some experiments, the transverse size and shape of the beam behind the exit foil were recorded with thin polymer plates including, in particular, astralon plates. The darkening of these plates when the beam passed through them was used a rough indication of the change in its configuration with the experimental conditions (see[4]).

The plasma density was measured by determining the absorption of 2, 4, 8, 13, and 30 mm radiation and with the aid of an 8-mm microwave interferometer. The plasma density distribution over the transverse cross section was also examined qualitatively with the aid of the plasmoscope 13 described in[5].

The transverse plasma pressure was recorded by four external single-turn diamagnetic probes 9 which had a diameter of 13 cm and were located at distances of 35, 90, 140, and 190 cm from the entrance foil. The probes were connected to integrating circuits with an integration constant RC $\sim$ 1 μsec. The signal from the diamagnetic probes was recorded with oscillographs with a pass band of 60 MHz. The time resolution of the diamagnetic probes was better than 10 nsec.

3. PASSAGE OF THE BEAM THROUGH THE VACUUM CHAMBER

When the beam is injected into the vacuum chamber (residual pressure 10^{-6} Torr), the total energy Q transmitted through the tube (measured by the calorimeter) and the exit beam current amplitude I_{ex} are found to depend strongly on the external magnetic field H. When H = 0, the current and the total energy of the beam at the end of the tube are zero, and the beam is not transmitted. When the magnetic field is introduced, the beam begins to pass through the vacuum tube. As the magnetic field increases, the energy transported by the beam and the current amplitude at first increase and then for H $\gtrsim$ 5 kOe they no longer depend on the magnetic field. The function Q(H) is shown in Fig. 2.

When the initial voltage on the cathode of the accelerator is 1 MV, the energy transported by the beam for H $\gtrsim$ 5 kOe is, on the average, 70 J. The amplitude of the output beam current is then $\sim$3 kA (see Figs. 3a and b). This is in satisfactory agreement with the critical current determined by applying an electrostatic bias against the beam. Elementary calculations (see[6]) show that in the case of a cylindrical return current lead of radius R which is much greater than the beam radius r_b, the critical current is given by[3]

$$I_{crit} \approx \frac{mc^3(\gamma_0^{1/3}-1)^{3/2}}{e[1+2\ln(R/r_b)]}, \qquad (1)$$

where $\gamma_0 = 1 + E_0/mc^2$ and E_0 is the kinetic energy of the beam immediately after the entrance foil. Substituting
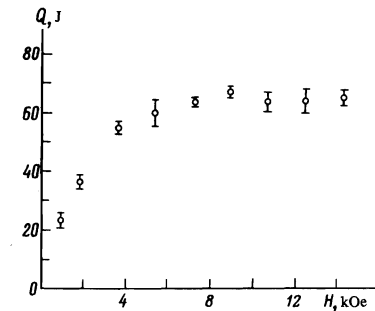
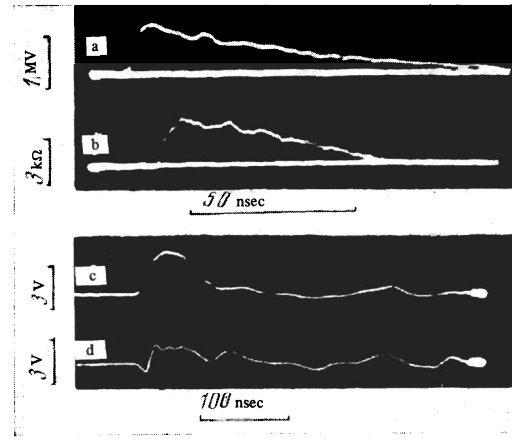FIG. 2. Energy transported by the beam in vacuo as a function of magnetic field.

FIG. 3. Typical oscillograms: a—voltage on the accelerator cathode, b—beam current at exit from the installation; the delay of the beam is connected with the transit of the electrons through the vacuum chamber, c,d—integrated signals from the first and second diamagnetic probes; the voltage of 1 V corresponds to $W_\perp \approx 5 \times 10^{16}$ eV/cm for H = 7 kOe. Conditions: vacuum, H = 7 kOe.

$\gamma_0 \approx 3$ and ln $(R/r_b) \approx 2$ in (1), we find that $I_{crit} \approx 4$ kA, which is a little higher than the observed critical current.[4] This discrepancy can be partially explained by the effect of induced emf due to the fact that the beam is not completely time-independent and by the reduction in the longitudinal momentum of beam electrons due to scattering in the entrance foil (the angular spread $\overline{(\theta_0^2)}^{1/2}$ of the $\sim$ 1 MeV beam in the 50-μ titanium foil was of the order of 15—20°).

When the beam passes through the vacuum chamber, the diamagnetic probes record signals with a rise time of 15—20 nsec and length roughly equal to the duration of the beam (see Figs. 3c and d). These signals can be interpreted as being due to beam diamagnetism.

The diamagnetic signal from the beam in the vacuum chamber is due to two effects. First, it is due to the transverse momenta $p_\perp$ of the beam particles. The corresponding contribution to the transverse pressure is

$$\mathscr{P}_\perp' = \frac{1}{2}n_b\overline{p_\perp v_\perp} = \frac{n_b}{2}\frac{\overline{p_\perp^2}}{m\gamma}.$$

Secondly, there is the electrostatic repulsion between the beam particles, and the corresponding contribution to the pressure is

$$\mathscr{P}_\perp'' = \pi r^2 e^2 n_b^2/\gamma^2,$$

(the factor $1/\gamma^2$ represents partial compensation of the electrostatic repulsion by magnetic compression). In view of the conservation of the adiabatic invariant, $p_\perp^2/H$ = const, we may write

$$\mathscr{P}_{\perp}' \approx \frac{n_b}{2} \frac{\overline{p_{\perp 0}^2}}{mk\gamma} = \frac{n_b p_0^2 \overline{\theta_0^2}}{2mk\gamma} = n_b mc^2 \frac{(\gamma_0^2-1)\overline{\theta_0^2}}{2\gamma k},$$

where k is the mirror ratio and the subscript zero labels the corresponding quantities on the entrance foil (in the mirror).

The value of γ inside the installation is, in general, different from γ_0 (because of the electrostatic deceleration in the beam). In our experiments, the beam current was nearly critical, in which case, it is readily shown that $\gamma = \gamma_0^{1/3}$, i.e.,

$$\mathscr{P}_{\perp}' = n_b mc^2 \frac{(\gamma_0^2-1)\overline{\theta_0^2}}{2\gamma_0^{1/3}k}.$$

The experiment yields directly the quantity

$$W_{\perp} = 2\pi \int (\mathscr{P}_{\perp}' + \mathscr{P}_{\perp}'') r\,dr = W_{\perp}' + W_{\perp}''$$

($W_{\perp}$ is expressed in terms of the change in the magnetic flux $\Delta\Phi$, i.e., $W_{\perp} = H\Delta\Phi/4\pi$). The components $W_{\perp}'$ and $W_{\perp}''$ can be expressed in terms of the beam current, as follows:

$$W_{\perp}' = \frac{mcI_b}{e} \frac{\gamma_0^2-1}{(\gamma_0^{1/3}-1)^{1/3}} \frac{\overline{\theta_0^2}}{2k}, \qquad (2)$$

$$W_{\perp}'' = \frac{I_b^2}{2c^2(\gamma_0^{1/3}-1)}. \qquad (3)$$

Substituting $I_b \approx 3000$ A and $\gamma_0 \approx 3$ in (3), we obtain $W_{\perp}'' \approx 2 \times 10^{16}$ eV/cm. Measurements yield $W_{\perp} = 6 \times 10^{16}$ eV/cm, i.e., $W_{\perp}' \approx 4 \times 10^{16}$ eV/cm. If we now substitute $I_b \approx 3000$ A, $\gamma_0 \approx 3$, k = 1.7 in (2), we find that the angular spread of the beam is $(\overline{\theta_0^2})^{1/2} \sim 0.25$ which, for this particular experimental accuracy, can be regarded as being in agreement with the estimate of the angular spread of beam particles in the titanium foil, given above.

We now return to the explanation of the function Q(H) in Fig. 2. It is readily seen that the condition for the transverse equilibrium of the beam $H^2/8\pi \gtrsim \mathscr{P}_{\perp}$ is satisfied even for H $\sim$ 0.5 kOe, i.e., the observed break on the Q(H) curve cannot be connected with transverse equilibrium of the beam. It is more likely that the function Q(H) shown in Fig. 2 is due to the reduction in the angular divergence of the beam in the diode gap of the accelerator when the magnetic field is increased. The magnetic field H $\approx$ 5 kOe corresponds to the situation where the angular divergence in the diode becomes less than the angular spread in the entrance foil, so that the subsequent increase in the magnetic field no longer leads to an improvement in the angular characteristic of the beam at entrance into the vacuum chamber.

When the transmission of the beam through the vacuum chamber in the presence of the magnetic field was investigated, it was found that there was strong radiation in the range between 10 and 40 GHz. Preliminary studies of the spectrum of this radiation with a quasioptical spectrometer and the postcritical waveguide method showed that the radiation spectrum was very dependent on the magnetic field. This radiation can be interpreted as the cyclotron radiation from the beam of relativistic electrons. However, the absolute intensity of this radiation is higher than the predicted intensity of cyclotron radiation from the beam with the given angular spread and particle density. The reason for this discrepancy may be the presence of inhomogeneities in the beam density with scales smaller than the Larmor radius r_H of the electron. Such inhomogeneities will lead to the

appearance of coherent cyclotron radiation whose intensity is higher roughly by a factor of $r_H^3 n_b (\Delta n_b/n_b)^2$ than that of the incoherent cyclotron radiation. Since $n_b \sim 3 \times 10^{11}$ cm^{-3} and $R_H \sim 0.5$ cm, we find that even for a very low level of inhomogeneity the gain is quite large. The reason for the appearance of the random inhomogeneities in the beam density may be the bursting of microspikes during the emission of electrons from the cathode. We note that the above mechanism is only a hypothesis and requires further experimental verification.

4. PASSAGE OF THE BEAM THROUGH PLASMA

The passage of the beam through the plasma was investigated mainly for magnetic fields H $\gtrsim$ 3 kOe. It was found that the beam energy recorded by the calorimeter at the end of the installation for a given magnetic field was very dependent on the density of the preliminary plasma. This was noted in[1] and in our previous paper,[3] the results of which are shown in Fig. 4a. It is clear from this figure that for n = $10^{12}-10^{13}$ cm^{-3} the beam loses 50,—70% of its initial energy. For n $\gtrsim 10^{13}$ cm^{-3}, the energy losses are substantially lower, and for n $\sim 10^{14}$ cm^{-3} they are no longer detectable against the spread of the experimental points.

Analogous measurements performed during the operation of the accelerator, which are typical for our experiments, are shown in Fig. 4b. In this case, more energy is transmitted through the dense plasma (n $\gtrsim 10^{13}$ cm^{-3}) than through the vacuum, and this is connected with the increase in the injection current over and above the limiting vacuum value I_{crit} (in the previous experiments,[3] the injection current was close to the critical value). The amplitude of the output beam current for n $\sim 10^{14}$ cm^{-3} is 5—5.5 kA and is appreciably greater than I_{crit}. The improvement in beam transmission in the presence of dense plasma is connected with charge and current neutralization of the beam.

The polymer plates were used to demonstrate that after passing through the vacuum the output beam has a symmetric form with a diameter of ~ 2.5 cm (Fig. 5a). When the beam passes through the plasma it may appreciably deflect and, at the same time, broaden (generally speaking, nonuniformly both in the radial and azimuthal directions). The beam is particularly strongly broadened and deflected for densities $10^{12}-10^{13}$ cm^{-3} (Fig. 5b). Under these conditions, the beam spreading is so large that part of it may hit the walls of the vacuum
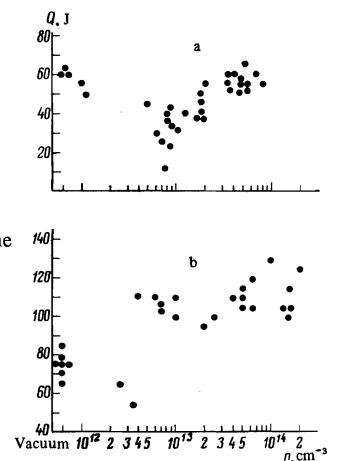

FIG. 4. Beam energy recorded by the calorimeter at exit from the system as a function of the density of the preliminary plasma (H = 7 kOe).

chamber. As a result, the calorimeter mounted at the exit will indicate large energy losses. This behavior of the beam may, to some extent, explain the energy losses and their dependence on plasma density reported in[1,3]. For high plasma densities ($n > 10^{13}$ cm^{-3}), one usually observes small beam spreading (Fig. 5c). An increase in the external magnetic field at constant plasma density then leads to a reduction in the beam spread.

This behavior of the beam can be due to two causes: either the reverse current in the plasma is not axially symmetric relative to the beam (because of inhomogeneities in the plasma conductivity) or for low densities ($n \lesssim 10^{13}$ cm^{-3}) the beam is macroscopically unstable.

Let us consider the first possibility in greater detail. In the case of inhomogeneities in conductivity, the reverse current will, in general, be shifted relative to the beam axis, and the magnetic field due to the reverse current will lead to transverse meandering of the beam. The situation is explained in Fig. 6 which illustrates the case when the plasma conductivity is different from zero only in a narrow cylindrical region which is displaced from the beam axis. The reverse current produces a magnetic field with circular lines of force. The effect of the external longitudinal magnetic field and the field due to the current is that the beam travels over a spiral which winds on the reverse current. It is readily seen that the result is a net shift of the beam relative to its initial position through a distance of 2Δ (Fig. 6), and the beam may hit the walls for large enough Δ. The pitch of the spiral in z is $2\pi(H/H_I)\Delta$, where H_I is the field due to the reverse current on the beam axis.

To get some idea about the possibilities of this kind of effect, let us consider the following numerical example: $\Delta = 2$ cm, H = 7 kOe. It is readily calculated that, under these conditions, the beam will shift over the length of the installation through a distance equal to the radius of the calorimeter (i.e., 3 cm) if the reverse current is ~900 Å. This amounts to ~15% of the beam current and may occur even for very low densities (see Fig. 7).

The pitch of the spiral and, correspondingly, the position of the beam leaving the installation, will vary in time because of the variation in the reverse current. The beam will then be recorded on the astralon plate in the form of a diffuse spot because the image on the plate represents the time-integrated picture. Naturally, in practice, the conductivity may be distributed more smoothly, but this does not affect the essence of the situation. We note merely that when the conductivity is very high, i.e., the inhomogeneity is relatively unimportant, the reverse current flows in the region occupied by the beam and completely compensates the beam current so that there is no beam deflection.

Studies of the transverse distribution of the plasma density with the aid of a plasmoscope in place of the entrance foil, showed that there were no clearly defined plasma inhomogeneities. It is not clear as yet whether the observed degree of inhomogeneity is sufficient to exclude the explanation of the beam spreading proposed above.

It will be seen from the ensuing discussion that the maximum energy release by the beam in the plasma is observed when the beam spreading is small.

In conclusion of this section, let us consider measurements of the total current in the plasma. These experiments showed that the beam current for plasma densities ~10^{12} cm^{-3} is very slightly compensated by the plasma current (Fig. 7b). When $n \sim 10^{13}$ cm^{-3}, beam current compensation is observed on the leading front. For a short time thereafter there is no compensation and, as the beam current falls, there is again an observable plasma current which flows in the same direction as the beam. There is even a stretching out of the total current as compared with the beam current (Fig. 7c). The rapid attenuation of the plasma current at the beginning of the beam and, consequently, the disappearance of compensation, may be connected with the appearance of anomalous resistance (the normal conductivity of plasma under

FIG. 5. Shape of the beam: a—vacuum, b—plasma with $n \sim 2 \times 10^{12}$ cm^{-3}, c—plasma with $n \sim 5 \times 10^{13}$ cm^{-3}.
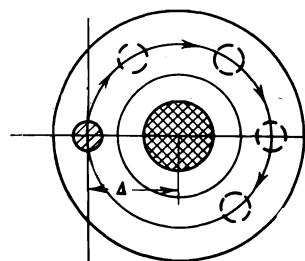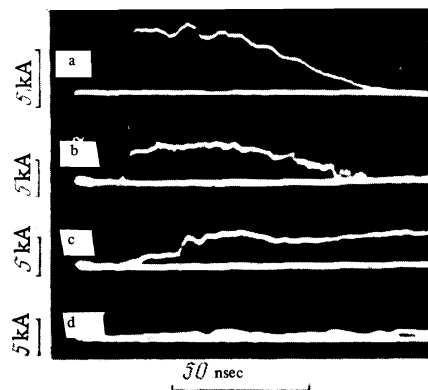

FIG. 6. Effect of inhomogeneity in conductivity on the transverse beam shift. The initial position is shown hatched. The region of high conductivity is shown doubly hatched. The circle represents the lines of force of the magnetic field. The broken circles show the beam positions at different distances from the entrance.

FIG. 7. Typical oscillograms: a—beam current at exit from plasma for $n \sim 10^{14}$ cm^{-3}; b, c, d—total current in the plasma for densities, respectively, ~10^{12}, ~10^{13}, and ~10^{14} cm^{-3}; H = 7 kOe.

these conditions is too high). As the beam current falls, the plasma conductivity again increases (possibly because of plasma heating), and the plasma current again appears and persists even longer than the beam. When $n \sim 10^{14}$ cm^{-3}, the beam current is compensated by the plasma current practically at all times (Fig. 7d), and this suggests that the plasma conductivity is sufficiently high.

5. PLASMA HEATING

When the beam passes through plasma, the diamagnetic signals increase in amplitude by a factor of 5—7 as compared with measurements performed in a vacuum, and their length substantially increases. Figure 8 shows typical oscillograms of signals from the diamagnetic probes. As a rule, the largest signal is observed in the first probe. In the third and fourth probes the signal is lower by a factor of 2—3. The difference between the signal amplitudes delivered by the different probes suggests that the observed diamagnetism is not determined by beam electrons trapped in the magnetic trap. If this were not so, then the equalization of the diamagnetic signals would occur during the time of transit of relativistic electrons through the trap which, under our conditions, amounts to a few nanoseconds. Consequently, it may be supposed that the diamagnetism is due to plasma heating.

The dependence of the energy content per unit length of the plasma column $W = nT_{\perp}S$ on the density of the preliminary plasma is shown in Fig. 9a[5]. It is clear that, up to plasma densities of 5×10^{13}—10×10^{13} cm^{-3}, there is a monotonic increase in the transverse plasma pressure. We note that the density at which maximum diamagnetism is observed is higher by almost two orders of magnitude as compared with the experiments in[1]. In

our experiments, the maximum diamagnetism was found to reach $nT_{\perp}S \approx 3.5 \times 10^{17}$ eV·cm^{-1}. If we suppose that the heating occurs only in the part of the plasma column through which the beam flows (S $\approx$ 7 cm^2) then we obtain $nT_{\perp} \approx 5 \times 10^{16}$ eV·cm^{-3}. If the plasma density is $n \approx 5 \times 10^{13}$ cm^{-3}, this corresponds to the heating of the plasma up to $T_{\perp} \approx 1$ keV. The energy stored in the entire plasma column after the passage of the beam, as determined from the diamagnetic measurements, amounts to 10—15% of the total beam energy.

After the beam has passed through partially ionized plasma, one observes additional ionization of the neutral particles. During this process the plasma density increases by a factor of two in a time of about 500 nsec. This ionization may be due to plasma electrons heated to a temperature of ~ 1 keV. This figure is in satisfactory agreement with the estimated temperature based on diamagnetic measurements.

The dependence of the transverse plasma pressure on the external magnetic field is shown in Fig. 9b. The field H was varied between 3 kOe and 15 kOe. The plasma pressure for given density was found to increase with increasing magnetic field.

It is important to note that at high plasma densities ($n \gtrsim 10^{14}$ cm^{-3}) there is a change in the nature of the diamagnetic signals (see Fig. 10). They begin to exhibit regular oscillations, and this is particularly clear for signals from the second and third probes. The frequency of these oscillations lies between 5 and 20 MHz and depends on the plasma density and the magnetic field. These oscillations are probably due to the excitation of radial magnetosonic oscillations in the plasma when the heating time is less than the time necessary for the propagation of the magnetic-field perturbation due to the diamagnetic expansion of the plasma. It is readily shown that this condition may be satisfied for plasma densities $n > 10^{14}$ cm^{-3} and magnetic fields H $\lesssim$ 5 kOe.

Let us now consider possible reasons for the observed plasma heating. As a result of Coulomb collisions, the plasma may be heated by the reverse current only to temperatures of 15—20 eV. For $T_e \gtrsim 20$ eV, Coulomb collisions become unimportant (their frequency is less than the reciprocal of the heating time). In principle, the reason for the heating may be the ion acoustic instability excited by the reverse current.[6] In point of fact, the condition for the excitation of the ion sound is

$$u > \alpha v_{Tc}(m/M)^{1/2}, \qquad (4)$$

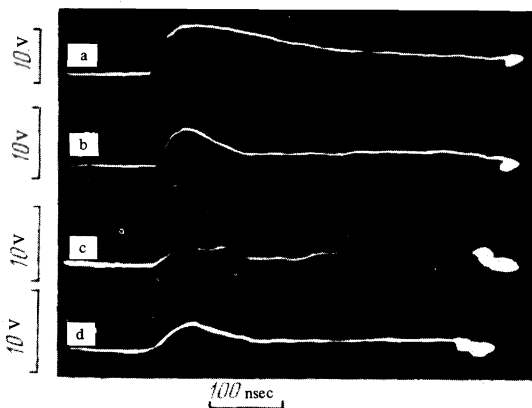where u is the directed velocity of the plasma electrons,

FIG. 8. Typical oscillograms of signals from the diamagnetic probes located at the following distances: a—35 cm, b—90 cm, c—140 cm, d—190 cm from the entrance foil. Conditions: H = 7 kOe, n $\approx$ 5 X 10^{13} cm^{-3}.
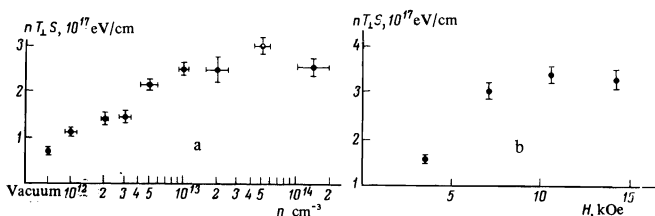
FIG. 9. Dependence of $nT_{\perp}S$ on the density of preliminary plasma for H = 7 kOe, and on the external magnetic field for n $\sim$ 5 X 10^{13} cm^{-3} (second probe, z_2 = 90 cm).
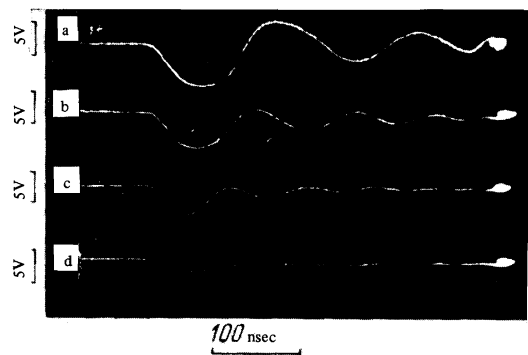
FIG. 10. Oscillograms of diamagnetic signals from the second (z = 90 cm) probe for high plasma density (n = 2 X 10^{14} cm^{-3}) and the following magnetic fields (in kOe): a—3.5, b—7, c—10, d—14.

Yu. I. Abrashitov et al.

v_{Te} is their thermal velocity, and α is a numerical factor which, in nonisothermal plasma ($T_e \gg T_i$) with isotropic electron distribution function, is of the order of unity. In the presence of current compensation $u = c(n_b/n)$ and condition (4) becomes

$$\frac{n_b}{n} > \alpha \frac{v_{Te}}{c}\left(\frac{m}{M}\right)^{1/4}. \tag{5}$$

This inequality was practically always satisfied in our experiments. Nevertheless, current compensation for $n > 5 \times 10^{13}$ cm^{-3} was almost complete, i.e., the ion-acoustic instability[7] did not lead to a restriction of the current velocity of the electrons to the critical level (4) with $\alpha = 1$. The possible reason for this phenomenon can be found in the deformation of the electron distribution function in the longitudinal electric field and the increase in α up to $\sim (M/m)^{1/2}$ (see [9,10]).

It follows from the foregoing that the ion-acoustic instability was apparently present in our experiments. However, simple estimates show that, at least under those conditions when almost total beam-current compensation occurred, the contribution of the reverse current to the plasma heating was unimportant. In fact, the energy ΔQ dissipated in the plasma by the reverse current I_r is

$$\Delta Q = \int_0^\infty I_r U_r\, dt, \quad U_r = \mathscr{L}\frac{d}{dt}(I_b - I_r), \quad \mathscr{L} = \frac{2L}{c^2}\ln\frac{R}{r_b},$$

where U_r is the induced emf and $\mathscr{L}$ is the inductance of the system. It is clear that

$$\Delta Q \lesssim \mathscr{L}\max|I_b|\max|I_r - I_b|. \tag{6}$$

Since $n \gtrsim 5 \times 10^{13}$ cm^{-3}, we have $\max|I_r - I_b| < 0.05\, I_b$ and it follows that $\Delta Q \lesssim 2.5$ J, i.e., the heating of the plasma by the reverse current under the conditions of good compensation is unimportant.

The foregoing discussion suggests that the heating of the plasma (at least for $n \gtrsim 5 \times 10^{13}$ cm^{-3}) is connected with the development of two-stream instability on Langmuir oscillations. The instability has a high growth rate $\sim (n_b/n)\omega_{pe}$ and is characterized by small fluctuation scales $\sim c/\omega_{pe}$ (see, for example, [11,12]). Estimates given in [1,2] show that, under the conditions of our experiment, the power released by the beam per unit plasma volume is given by

$$q(z) \sim \frac{mc^3 n_b \gamma_0}{L^*}\left(\overline{\theta_0^2} + \frac{z}{L^*}\right)^{-1/2},$$

where

$$L^* \sim \gamma_0^2\frac{c}{\omega_{pe}}\left(\frac{mc^2}{T_e}\right)^2\frac{8\pi n T_e}{H^2} \tag{7}$$

is the so-called relaxation length[8] (the beam loses roughly half its initial energy over the scale L*) and z is the distance from the entrance foil. The fraction of energy left by the beam in the plasma is given by

$$\xi = \frac{\int_0^L q(z)\, dz}{mc^3 n_b \gamma_0} \approx \frac{L}{L^*(\overline{\theta_0^2})^{1/2}}. \tag{8}$$

Substituting $n \approx 10^{14}$ cm^{-3}, $T_e \approx 1000$ eV, $H \approx 7$ kOe, $\gamma_0 \approx 3$, and $\overline{\theta^2} \sim 0.1$ in (7) and (8), we obtain $\xi \approx 0.1$ which is in adequate correspondence with the experimental data. The dependence of ξ on the plasma parameters is $\xi \propto H^2/n$ which is not inconsistent with the experimental data (for $n \gtrsim 10^{14}$ cm^{-3} for which Eqs. (7) and (8) are valid).

It is shown in [1,2] that, in the case of the relaxation of the beam on Langmuir oscillations, the relative beam energy loss ξ is roughly equal to the increase in the angular spread. Under our conditions, this means that the angular spread of the beam increases roughly by $\Delta\theta \sim 10°$. This corresponds to a very small increase in the transverse size of the beam ($\Delta r_b \sim 0.1$ cm).

The suppression of beam instability by plasma inhomogeneity, which was noted in [14], was probably absent from our experiment because of the high beam density.

In a recent paper, Breizman[15] analyzed the beam-relaxation mechanism connected with the excitation of short wave (scale $\lambda \sim c/\omega_{He}$) helicons. It was found that this mechanism may be very effective under certain conditions. However, in our experiment, it could hardly have played an appreciable role since, owing to the relatively small growth rate (Im $\omega \sim \omega_{He} n_b/n$) and relatively high group velocity [$v_g \sim c(\omega_{He}/\omega_{pe})^2$], the helicons are more likely to be transported out of the beam rather than develop (the condition $\tau \sim r_b/v_g \ll 1/$Im ω is satisfied).

In our view, therefore, the most important results of this work are as follows:

1. It has been established that a high-intensity relativistic electron beam produces collisionless plasma heating for plasma densities up to 2×10^{14} cm^{-3}. The heating efficiency under the optimum conditions is 10–15%.

2. The ion-acoustic instability and anomalous plasma resistance have very little effect on the dissipation of the beam energy for high plasma densities ($n > 5 \times 10^{13}$ cm^{-3}). The results of experiments in this density range are not inconsistent with the previously developed theory of beam relaxation on Langmuir oscillations.

3. Substantial axially nonsymmetric spreading of the beam at low plasma densities ($n < 10^{13}$ cm^{-3}) has been found. This effect is probably responsible for the previously established dependence of the beam energy loss on plasma density. [1,3]

---

1)The figure of 10% was not explicitly reported in [1]. Our estimate is based on the diamagnetic data given in [1].

2)We note that the calorimeter diameter (6 cm) was much greater than the beam diameter in the vacuum chamber (2.5 cm).

3)In our case, as has already been noted, the return current lead was in the form of four busbars but it is readily verified that allowance for this fact leads to the appearance of a small correction [$\sim(r_b/R)^4$] in (1). We note that (1) itself is accurate to within $\sim(2\, nR/r_b)^{-1}$.

4)We note that the injected current was roughly 5–6 kA (this will be clear from the experiments on the injection of the beam into a dense plasma, described below.) In the case of the vacuum, part of the current is returned to the accelerator. The reflection occurs over a distance of the order of the diameter of the reverse current lead from the entrance foil.

5)The quantity $nT_\perp S$ was determined from the maximum diamagnetic signal in the second probe. The signal produced by this probe corresponded approximately to the diamagnetism averaged over the length.

6)Attention was drawn to this effect for the first time in [7] and, subsequently, in [1,8].

[7)]The condition $\tau \, \text{Im} \, \omega \gtrsim 10$ (where τ is the beam length and $\text{Im} \, \omega$ is the instability growth rate) is satisfied for the ion-acoustic instability with a considerable margin: $\text{Im} \, \omega \approx \omega_{pi} \, (u/v_{Te}) \, (n_b/n) \approx 5 \times 10^8 \, \text{sec}^{-1}$ (for $n = 10^{14} \, \text{cm}^{-3}$, $n_b = 3 \times 10^{11} \, \text{cm}^{-3}$, $v_{Te} = 2 \times 10^9 \, \text{cm/sec}$), $\tau = 5 \times 10^{-8}$ sec, and $\tau \, \text{Im} \, \omega \approx 25$.

[8)]In contrast to [1] we do not include the factor T_i/T_e in (7). The importance of this was discussed in [13].

[1] A. T. Altyntsev, B. N. Breĭzman, A. G. Es'kov, O. A. Zolotovskiĭ, V. I. Koroteev, R. Kh. Kurtmullaev, V. L. Masalov, D. D. Ryutov, and V. N. Semenov, Plasma Physics and Controlled Nuclear Fusion Research 2, 309 (1971).

[2] B. N. Breĭzman, D. D. Ryutov, and P. Z. Chebotaev, Zh. Eksp. Teor. Fiz. 62, 1409 (1972) [Sov. Phys.-JETP 35, 741 (1972)].

[3] V. S. Koydan, V. M. Lagunov, V. N. Lukyanov, K. I. Mekler, and O. P. Sobolev, Proc. Fifth Europ. Conf. on Plasma Physics and Controlled Nuclear Fusion Research, Grenoble, 1972, p. 161.

[4] B. P. Sannikov, Tezisy simpoziuma po émissionnoĭ plazmennoĭ sil'notochnoĭ élektronike, Tomsk (Abstracts of a Symposium on High-Current Plasma Emission Electronics, Tomsk), 1973, p. 22.

[5] E. I. Dobrokhotov, A. V. Zharinov, I. N. Moskalev, and D. P. Petrov, Yad. Sintez 9, 143 (1969).

[6] L. S. Bogdankevich and A. A. Rukhadze, Usp. Fiz. Nauk 103, 609 (1971) [Sov. Phys.-Uspekhi 14, 163 (1971)].

[7] L. I. Rudakov, Zh. Eksp. Teor. Fiz. 59, 2091 (1970) [Sov. Phys.-JETP 32, 1134 (1971)].

[8] R. V. Lovelace and R. N. Sudan, Phys. Rev. Lett. 27, 1256 (1971).

[9] G. E. Vekshteĭn, D. D. Ryutov, and R. Z. Sagdeev, Zh. Eksp. Teor. Fiz. 60, 2142 (1971) [Sov. Phys.-JETP 33, 1152 (1971)].

[10] A. A. Vedenov and D. D. Ryutov, Vsb. Voprosy teorii plazmy (in: Problems of Plasma Theory), Atomizdat, 1972, Vol. 6, p. 3.

[11] Ya. B. Faĭnberg, V. D. Shapiro, and V. I. Shevchenko, Zh. Eksp. Teor. Fiz. 57, 966 (1969) [Sov. Phys.-JETP 30, 528 (1970)].

[12] B. N. Breĭzman and D. D. Ryutov, Zh. Eksp. Teor. Fiz. 60, 408 (1971) [Sov. Phys.-JETP 33, 220 (1971)].

[13] B. N. Breĭzman, V. E. Zakharov, and S. L. Musher, Zh. Eksp. Teor. Fiz. 64, 1297 (1973) [Sov. Phys.-JETP 37, 658 (1973)].

[14] B. N. Breĭzman and D. D. Ryutov, ZhETF Pis'ma Red. 11, 606 (1970) [JETP Lett. 11, 421 (1970)].

[15] B. N. Breĭzman, Proc. Sixth Europ. Conf. on Plasma Physics and Controlled Nuclear Fusion Research, Moscow, 1973, p. 491.

Translated by S. Chomet
136